https://doi.org/10.5194/nhess-2021-180
Preprint. Discussion started: 8 July 2021

Natural Hazards and Earth System Sciences
Discussions

Quantitative interpretation of risk potential of beach erosion due to coastal zone development

Changbin Lim[1], Taekon Kim[1], Sahong Lee[1], Yoon Jeong Yeon[1], Jung Lyul Lee[1,2]

[1]School of Civil, Architecture and Environmental System Engineering, Sungkyunkwan University, Suwon, 16419, Republic of Korea
[2]Graduate School of Water Resources, Sungkyunkwan University, Suwon, 16419, Republic of Korea

Corresponding author: Jung Lyul Lee (jllee6359@hanmail.net)

Abstract. Coastal erosion is more severe due to human-induced coastal zone development in addition to natural climate change. Anthropogenic development affecting coastal erosion is divided into three areas; watersheds, coastal waters, and coastal land areas. In this study, the ultimate effect of anthropogenic development on changes in the amount of sand, changes in the littoral drift, and changes in shoreline variability in these three planar areas is expressed as quantitative risk potential of beach erosion damage, defined as a change in the planar surface of the sand beach. The change in the amount of sand is due to the law of conservation of matter, and the littoral drift characteristic of sand is interpreted as a change in the main crest line at the breaking point, and the response characteristics of shoreline position is interpreted as change in the erodibility and recovery characteristics of beach sand. This quantitative method was applied to Bongpo-Cheonjin Beach of erosion grade D (frequency of erosion damage within 5 years) in Gangwon-do, Korea to identify the cause of erosion and evaluate the detailed applicability of this method. It was interpreted using a series of aerial photographs taken from 1972 to 2017 and survey data obtained from the erosion rating project started in 2010. In the erosion rating project, the GPS shoreline survey of 4 times per year and the sand sampling at the swash zones of base line at 150m intervals are mainly carried out. We showed the feasibility of methodology evaluating the risk potential for beach erosion proposed in this study, and it can be expected that this method will be applicable to eroded beaches elsewhere.

Key words: Littoral Cell, Equilibrium Shoreline, Beach Response, Grain Size of Sediments, Shoreline Survey.

1 Introduction

In recent years, erosion of sandy beaches has intensified in many countries due to the complex effects of climate change (i.e. global sea-level rise), reduced coastal sediment budgets (e.g. due to changes in watershed environment), and deterioration of coastal environments (e.g. caused by artificial structures and human interference). More seriously, the scale of development to coastal environments has threatened beach safety through (1) changes in nearshore wave fields following the installation of harbor structures, (2) permit of inappropriate large-scale reclamation without preventive measures, (3) decrease in beach buffer width with the construction of roads and infrastructure, and (4) reduction in the upstream sediment supply.

https://doi.org/10.5194/nhess-2021-180
Preprint. Discussion started: 8 July 2021


Natural Hazards and Earth System Sciences Discussions

Coastal erosion is often accompanied by environmental and social problems. In many developed countries, including South Korea, urbanization on narrow coastal strips has caused damage to the natural coastal environments. However, because it is difficult to correctly identify the risk to erosion and logically deduce their mechanisms, many eroding beaches have been over-protected, causing high countermeasure cost and further damage to downdrift coasts. Therefore, it is imperative to evaluate the existing regulations for beach erosion control and guidelines for coastal development, as well as incorporate environmental impact assessments into a comprehensive licensing system. To achieve these goals, an appropriate method is required to identify the risk to beach erosion and determine the most appropriate strategy.

Coastal erosion is divided into erosion caused by a decrease in the total amount of sand on the sandy beach, and erosion caused by a decrease in the beach width due to longshore and cross-shore sedimentations while the amount of sand is maintained. The former occurs when there is an imbalance in the sand budget and the amount of incoming sand becomes smaller than the amount of outflow, while the latter is caused by (1) a decrease in the beach width in the region where the equilibrium shoreline retreats due to wave field changes which generate transport of longshore sediment, and (2) a decrease in the beach width in the section where the equilibrium shoreline retreats due to a change in the wave field, or a temporary retreat of the shoreline due to the influence of sand suspension and offshore transport under the storm wave incidence. Although the physical processes that cause erosion are characteristically subdivided as described above, independent research on each erosion process has been actively conducted, but it is rare to find out the cause of erosion by quantitatively evaluating all erosion processes. The following is a summary of research contents on the budget analysis, longshore sediment transport, and cross-shore sediment transport process that contributed to the quantitative recognition of this study.

The beach maintains its current volume as the sediment budget is balanced. Therefore, it is essential to analyze it by dividing it into littoral cells, which are the zones that affect the sedimentation budget as done by Inman and Jenkins (1984) and Bray et al. (1995) and so on. When the amount of sediment discharge into or leaving in the littoral cell changes, a new equilibrium volume of sand is established in the beach accordingly (Dolan et al., 1987; Kana and Stevens, 1992; Pethick, 1996; Cooper, 1997; Cooper and Pethick, 2005). Therefore, the amount of sediment entering into the beach from the river and the amount of sediment leaving into the open sea by the continuous wave action should be interpreted as the main impacts of the sediment budget. For example, a decrease in sediment discharge due to the construction of dams in rivers (Foley et al., 2017; Warrick et al., 2019) or an increase in sand loss due to sand mining (Edward et al., 2006) causes gradual shoreline retreat. And Lee and Lee (2020) proposed an equation to calculate the beach width according to the law of mass conservation by placing variables representing two main factors about sediment budget.

It is assumed that the longshore sediment transport alters the feature of shoreline, but does not change the quantity of sand in the littoral cell. Thus, this results in deposition in some areas, but at the same time, erosion in some areas. Numerous observations and studies have been conducted to estimate the correlation of longshore sediment transport rate to wave and sand environments (Komar and Inman, 1970; CERC, 1984; Kamphius, 2002; Bayram et al., 2007). However, it is still mostly dependent on the empirical models in estimating the equilibrium shoreline in the vicinity of harbor breakwaters or coastal structures. Among them, the parabolic bay shape equation (PBSE; Hsu and Evans, 1989) has been recognized for its utility in

https://doi.org/10.5194/nhess-2021-180
Preprint. Discussion started: 8 July 2021


Natural Hazards and Earth System Sciences Discussions

many countries and is being used for coastal management (USACE, 2002; Herrington et al., 2007; Bowman et al., 2009; González et al., 2010; Silveira et al., 2010; Yu and Chen, 2011; Anh et al., 2015; Thomas et al., 2016; Ab Razak et al., 2018a & 2018b). Recently, Lim et al. (2021) applied the empirical equation of parabolic equilibrium shoreline of Hsu and Evans (1989) to the polar coordinate fitting the shoreline to prove its versatility for general sand beaches.

Lastly, cross-shore sediment transport causes morphological changes in the beach profile due to the wave, causing shoreline retreat. Much work has been done to interpret geomorphological phenomena (Swart, 1974; Wang et al., 1975; Wright et al., 1985; Miler and Dean, 2004; Yates et al., 2009; Montaño et al., 2020). Recently, Kim (2021) proposed a method of estimating the erosion width by frequency through statistical analysis of GPS shoreline observation data observed by season for more than 10 years. Kim (2021) also devised the concept of horizontal movement of suspended sediments and applied a wave scenario model to analyze the response relationship between the convergent MSL of Yates et al (2009).

In this study, the ultimate planar area of beach erosion occurring in the beach according to the anthropogenic factors that induce beach erosion is obtained, and the process of estimating the consequence of beach erosion damage corresponding to the area of the erosion zone that is damaged is introduced. In addition, a method of estimating the frequency according to the beach erosion width from the survey data of shoreline variability and, finally, a method of quantitatively estimating risk potential is presented. The risk potential is expressed in terms of the beach planar area, and it is ultimately equivalent to the area of erosion damage received from development activities, although it is unknown when the impact will be completed.

The *encroachment accumulation curve*, which calculates the area of the encroached section of the beach according to the erosion width, corresponds to the vulnerability curve. Here, the erosion width corresponds to the hazard, and the erosion width from the average coastline due to anthropogenic development includes the development of watershed areas, coastal waters, and coastal land areas. The erosion width is accomplished through three different planar areas; (1) the planar area of the beach that is ultimately reduced due to the development of watershed areas, (2) the planar area that is ultimately eroded due to the change in the wave field due to the development of the coastal waters, and (3) the planar area that is temporarily eroded due to the occurrence of cross-shore transport due to the periodic high wave incidence. Assuming that the total eroded planar area obtained in this way evenly affects the entire beach length except for a part of the deposition section due to shoreline deformation, it is divided by the beach length L to finally obtain the beach erosion width corresponding to the hazard strength. The methodology presented in this study is applied to the Bongpo-Cheonjin Beach, South Korea, a coast with a high risk of erosion, and the validity of the methodology is verified.

After a brief introduction in section 1, section 2 of this paper discusses the erosion risk potential using the concept of the *encroachment accumulation curve*. Section 3 of this paper discusses methods for quantifying three erosion potential mechanisms: (1) sediment reduction from an updrift river, (2) longshore sediment deposition causing beach erosion following harbor breakwater construction in the downdrift region, and (3) shoreline retreat due to cross-shore sediment during high waves. The combined quantitative results are then applied to Bongpo-Cheonjin Beach, with the support of aerial photographs taken between 1972 and 2017, 37 sets of seasonal shoreline survey data collected during 2008–2017 and NOAA's wave data, with results presented are graphically in Sect. 4. Temporal changes of the individual potential are discussed in Sect. 5. Finally,

https://doi.org/10.5194/nhess-2021-180
Preprint. Discussion started: 8 July 2021


Natural Hazards and Earth System Sciences Discussions

concluding remarks are given in Sect. 6. It is expected that this quantitative method for identifying the risk to beach erosion could be applied to similar coastal environments on the eastern coast of the Korean Peninsula, as well as elsewhere in the developing and developed countries.

2. Beach Erosion Risk

Recently, in several countries including the United States and Europe, the analysis of coastal impact caused by extreme events such as hurricane is increasing (eg Beven II et al., 2008; Kunz et al., 2013; Van Verseveld et al., 2015; Spencer et al., 2015). Sanuy et al. (2018) established an erosion risk assessment method based on the Bayesian network, and searched for a method to reduce erosion by applying it to beaches located in the Mediterranean. In addition, many studies have been conducted to evaluate coastal risks through analysis and prediction of various physical phenomena and effects using numerical models (eg Roelvink et al., 2009; McCall et al., 2010; Harley et al., 2011; Roelvink and Reniers, 2012).

However, most risk assessment methods are not only focused on extreme events, but also require numerous data and techniques, so it is not practical for coastal managers to apply them to real fields for coastal erosion management purposes. Therefore, in this study, we suggest a method to assess the ultimate risk (risk potential) of erosion damage using a set of minimal data such as existing aerial photos or techniques estimating the sediment load reduction due to watershed development, shoreline survey data, sea area development and deployment plan, and encroachment status without additional field observation at the time when coastal development is planned.

2.1 Definition of beach erosion risk

Risk is defined as the time-averaged amount of damage, and the evaluation is possible through time domain, frequency domain, and probability domain analysis. In general, in the expression of the frequency domain, risk R is defined as the product of consequence C and frequency F as shown in the following equation,

$$R = CF \quad (1)$$

The risk potential (ultimate risk) in this study is the value corresponding to the consequence C of the right side of Eq. (1), and is defined as the planar area ultimately damaged by erosion according to the development of watersheds, land, and coast. The sand buffer zone does not cause damage even if erosion occurs, and is excluded in the damage evaluation as a section that recovers over time. And the frequency F on the right side of Eq. (1) corresponds to the frequency of erosion from the equilibrium shoreline to the erosion width. This value represents the erosion vulnerability of the beach and is obtained under the assumption that there exists erodible sandy beach.

https://doi.org/10.5194/nhess-2021-180
Preprint. Discussion started: 8 July 2021


Natural Hazards and Earth System Sciences Discussions

125 **2.2 Risk potential of beach erosion**

Quantitative estimation of Consequence C is made from the analysis of all factors affecting the planar area change of the beach. As already mentioned in the introduction, coastal erosion occurs due to imbalance in the sand budget, changes in wave fields, and shoreline retreat due to high wave incidence. As such, the physical process that causes erosion is characteristically subdivided, so the erosion consequence C is calculated through the sum of the independently calculated erosion planar areas.
130 (1) The planar area that is reduced due to the lack of sand budget is called the *sediment budget reduction potential* A_c, (2) the planar area newly deposited as longshore sediment transport due to the change of the wave field is called the *longshore sediment deposition potential* A_d, and (3) the planar area that is retreated from the shoreline due to the high wave incidence is called the *cross-shore sediment retreat potential* A_e. The erosion width is measured shoreward with respect to the equilibrium shoreline. For the previous two cases, the concept of frequency is not established, but for the last, beach erosion due to high
135 wave incidence, the frequency F is estimated through the statistical analysis of shoreline survey data.
Since the sum of the planar areas of erosion includes a buffer zone in which no damage occurs, the value itself does not become a risk potential and is obtained through an *encroachment accumulation curve* according to the erosion width from the equilibrium shoreline. A sandy buffer zone indicates an area unaffected by storm/high waves for a specific number of years, thus where sediment is recovered as it is after storms. The following introduces the method of obtaining the erosion width
140 from the equilibrium shoreline from the erosion planar area and the method of extracting the *encroachment accumulation curve*.
It can be assumed that the total planar area of erosion affects the entire length of the beach, excluding a short part of the deposition section due to shoreline deformation, and thus dividing by the length of the beach L, the shoreline retreat W_t can be obtained as follows.

145 $$W_t = W_c + W_d + W_e \quad (2)$$

The right-hand side of Eq. (2) includes the effect of (1) reduction in sediment budget from river supply W_c, (2) alongshore sediment deposit due to harbor breakwater construction W_d, and (3) cross-shore sediment retreat by high waves W_e which has different values depending on the frequency. When W_t is calculated, as shown in Figure 1, the overall erosion consequence C_t can be obtained from the *encroachment accumulation curve* that accumulates the area to be damaged by the hinterland
150 development of the buffer section based on the average shoreline.

https://doi.org/10.5194/nhess-2021-180
Preprint. Discussion started: 8 July 2021

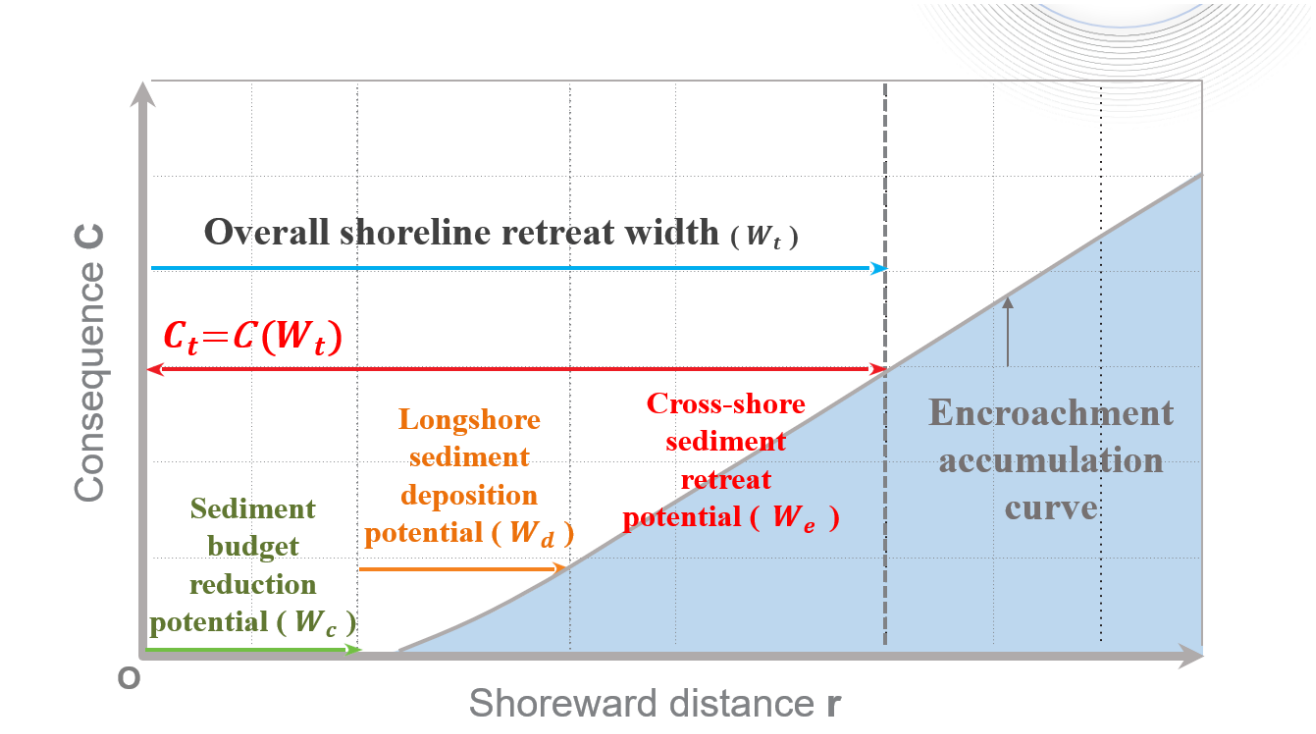

Figure 1: Evaluation of risk consequence components by using an encroachment accumulation curve.

The following introduces the method of extracting an *encroachment accumulation curve*. It is a curve that accumulates the encroached area with respect to the shoreward distance from the average shoreline. If the circle that best fits the current average shoreline is obtained, the center of the circle O can be obtained. As shown in Fig. 2, the average shoreline is located at R_o from the origin of the circle, and the encroached boundary (red dashed line in Fig. 2) is located at R_{ec} from the origin. Of course, each angle α has a different value depending on the encroached aspect. Therefore, if R_o and R_{ec} are determined for each angle α, the *encroachment accumulation curve* is obtained by the following equation according to the shoreward distance r from the average shoreline.

$$C(r) = \int_{\alpha=0}^{\alpha=\alpha_e} \delta(\alpha)[(R_o(\alpha) + r) - R_{ec}(\alpha)]d\alpha \quad (3)$$

where,

$$\delta(\alpha) = 1 \qquad \text{for } R_o(\alpha) + r > R_{ec}(\alpha) \quad (4a)$$

$$\delta(\alpha) = 0 \qquad \text{for } R_o(\alpha) + r < R_{ec}(\alpha) \quad (4b)$$

https://doi.org/10.5194/nhess-2021-180
Preprint. Discussion started: 8 July 2021

Natural Hazards and Earth System Sciences
Discussions

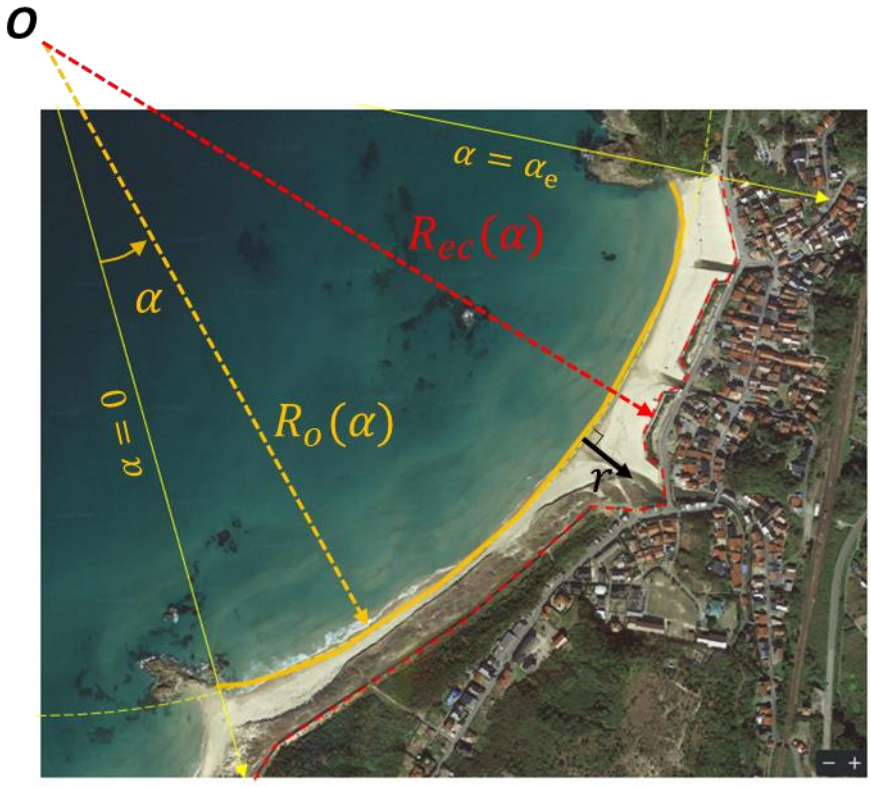

Figure 2: Conceptual diagram of encroachment accumulation curve for the total erosion potential on image courtesy of © Google Earth.

2.3 Calculation process of the beach erosion risk

In Eq. (2), r is the shoreward coordinate from the average shoreline, and if shoreline retreat W_t of Eq. (2) is substituted for r, the erosion width invades the encroachment zone and the planar area where damage occurs is obtained. This area corresponds to a consequence C of Eq. (1), where frequency F can be regarded as a one-year frequency in the case of W_c and W_d, on the other hands, W_e depends on the frequency of high wave incidence. Therefore, if concepts of the erosion potential and the *encroachment accumulation curve* are applied, the risk in Eq. (1) is expressed as the following equation.

$$R(r) = C_l + C_e(r)F_e(r) \quad (5)$$

where $C_l = C(W_c + W_d)$ and $C_e = C(W_t) - C_l$.

In general, W_c and W_d mean the ultimate retreats of the future shoreline from the current shoreline position, respectively and are considered smaller than W_e. Therefore, if the buffer section is sufficient, C_l hardly occurs, so the first term on the right side of Eq. (5) is judged to be insignificant. The methodology of quantitatively estimating the variables appearing in Eq. (5) is described in Sect. 3.

https://doi.org/10.5194/nhess-2021-180
Preprint. Discussion started: 8 July 2021


Natural Hazards and Earth System Sciences
Discussions

3. Quantitative Interpretation

3.1 Sediment budget reduction potential

The sediment budget reduction potential is defined as the reduction in the planar beach area mainly followed by the lack of river sediment load due to the watershed development. Applying the law of conservation of matter to the beach of the littoral cell (Lee and Lee, 2020), it can be expressed as

$$\frac{dV}{dt} = Q_{in} - Q_{out} \tag{6}$$

where Q_{in} is the rate of sediment discharge into the beach and Q_{out} is the sediment discharge leaving from the beach. Representing Q_{in} is the amount of sediment from the river and representing Q_{out} is the sediment discharge lost to the sea due to the action of waves. If we express the loss rate due to wave action as a function of the constant value of sand loss rate K, the following equation is established:

$$\frac{dV}{dt} = Q_{in} - KV \tag{7}$$

where beach volume V can be expressed as the product of the vertical height of littoral zone D_s and beach planar area A, assuming that D_s, the sum of berm height and closure depth, is constant along the beach. The sand loss rate K can be calculated from the sediment amount entering the beach. Therefore, Eq. (7) becomes the following equation:

$$\frac{dA}{dt} = \frac{1}{D_s} Q_{in} - KA \tag{8}$$

A detailed description of the seaward loss of suspended sand due to wave action, Q_{out}, expressed in KV, is presented in Lee and Lee (2020). If Eq. (8) is applied to the steady state and Q_{in} decreases by α due to watershed development, forestation, or river maintenance projects, it also decreases by α in beach area, as in the following equation;

$$\frac{(1-\alpha)}{Ds} Q_{in}^{o} - K(A^{o} - \Delta A) = 0 \;\rightarrow\; \Delta A = \alpha \frac{1}{KDs} Q_{in}^{o} = \alpha A^{o} \tag{9}$$

Here, the superscript 'o' corresponds to the beach area before development. This reduced beach area ΔA is defined as the *sediment budget reduction potential* A_c (Fig. 3). Assuming that A_c is uniformly spread over the entire embayment with a curved length of L_c, then beach width reduction W_c can be estimated by

$$W_c = \frac{A_c}{L_c} . \tag{10}$$

https://doi.org/10.5194/nhess-2021-180
Preprint. Discussion started: 8 July 2021

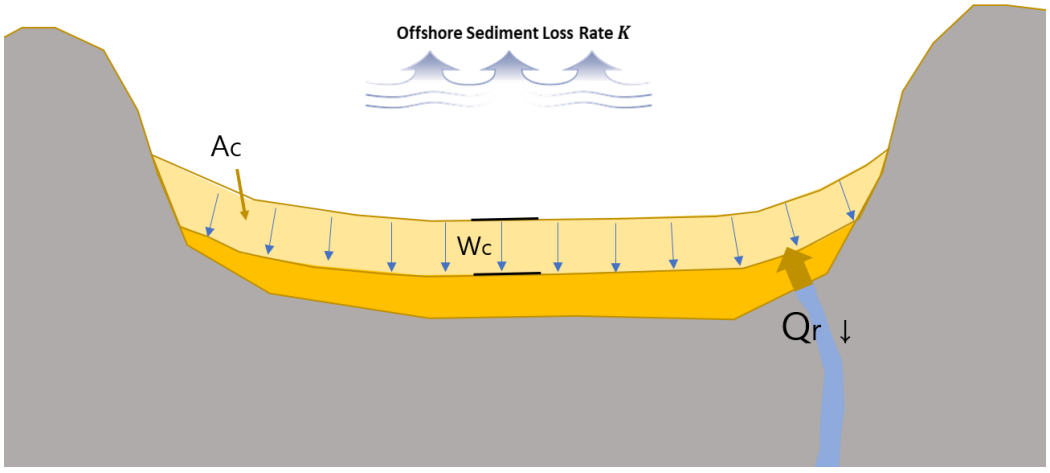

Figure 3: Conceptual diagram of the sediment budget reduction potential.

3.2 Longshore sediment deposition potential

The longshore sediment deposition potential is defined as the planar area of the depositional zone caused by the deformation of the shoreline due to wave field changes. The parabolic bay shape equation (PBSE; Hsu and Evans, 1989) is applied to delineate the shoreline feature in static equilibrium and simply recognize the ultimate bay shape formed after the construction of a harbor breakwater. This equation can be used to define two adjoining regions with a common tangent at the downdrift control point *E* (Fig. 4):

$$R(\theta) = \frac{a}{\sin\beta}\left[C_0 + C_1\left(\frac{\beta}{\theta}\right) + C_2\left(\frac{\beta}{\theta}\right)^2\right] \qquad \text{for } \theta \geq \beta \qquad (11a)$$

$$R(\theta) = \frac{a}{\sin\beta} \qquad \text{for } \theta \leq \beta \qquad (11b)$$

where R_0 is the length of the control line (*FE*) joining the parabolic focus (*F*; wave diffraction point) and the downdrift control point (*E*), $R(\theta)$ is the radius from the focus to a point *Q* on the equilibrium shoreline, a is the perpendicular distance from the wave crest baseline to point *E*, β is the angle between the wave crest baseline and the line joining the focus and the control point, θ is the angle between the wave crest baseline and the line connecting *F* and *Q*, and C_0, C_1 and C_2 are the coefficients provided by Hsu and Evans (1989). The approximate expression of the PBSE can be given as,

$$R(\theta) \cong \frac{\beta}{\sin\beta}\frac{a}{\theta} \qquad (12)$$

https://doi.org/10.5194/nhess-2021-180
Preprint. Discussion started: 8 July 2021

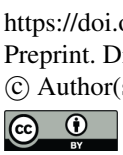

Natural Hazards and Earth System Sciences
Discussions

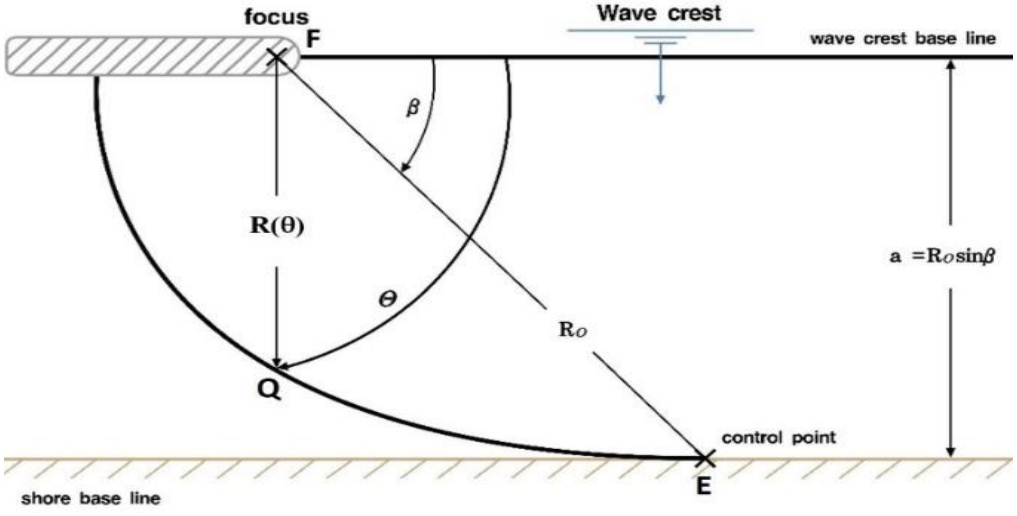

Figure 4: Sketch of parabolic bay shape equation and relevant geometric parameters.

The shoreline change arising from bay shape formation predicted by the PSBE causes alongshore sediment movement, results in simultaneous downdrift erosion and updrift accretion. Recently, Lim et al. (2021) extend the applicability of the PBSE with polar coordinates to concave coasts. In the present case, the actual equilibrium shoreline can be estimated by shifting the downdrift segment of the predicted bay shape landward, parallel to the existing shoreline, and equating the accreted area (A_d^+) with the eroded area (A_d^-), as shown in Fig. 5. The accreted area, which is *the longshore sediment deposition potential*, can also be obtained from Eq. (13),

$$\frac{A_d}{a^2} = \frac{1}{2}[\cot(\pi - \beta') + \cot\beta] + \frac{1}{2}\frac{\beta}{\sin\beta}\left(\frac{1}{\pi-\beta'} - \frac{1}{\beta}\right) \quad (13)$$

In Eq. (13) and Fig. 5, β' is the angle between the headland (i.e., the breakwater tip) and coastal structure (e.g., harbor breakwater) or longshore sediment control facilities (e.g., groin). For application, Eq. (13) can be approximated as,

$$\frac{A_d}{a^2} \cong \frac{28.8}{\beta'} - 0.004\beta \qquad \text{(unit: degree)} \quad (14)$$

Then, the extent of shoreline retreat (W_d) can be calculated from dividing the accretion area A_d by L_d, which is the length from the focus point to the farthest point on the downdrift beach or the shoreline length in the erosion section (Fig. 5),

$$W_d = \frac{A_d}{L_d} \quad (15)$$

https://doi.org/10.5194/nhess-2021-180
Preprint. Discussion started: 8 July 2021

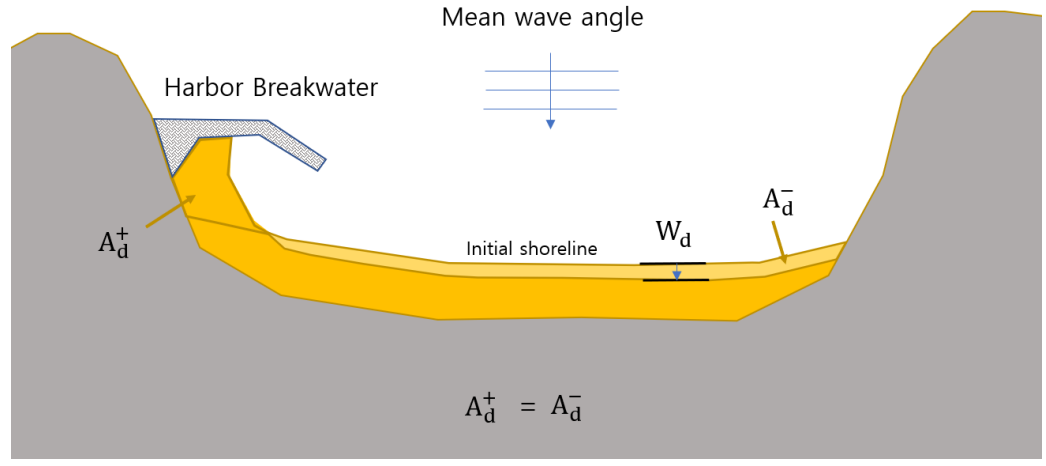

235 **Figure 5: Longshore sediment deposition potential caused by shoreline deformation.**

3.3 Cross-shore sediment retreat potential

The cross-shore sediment retreat potential is defined as a planar beach area that is temporarily eroded by high wave incidence. Figure 6 shows that the beach profiles have a relatively constant value at a certain closure depth but have continuously changing values in the vicinity of shoreline position. Shoreline survey data performed four times a year show that the distribution follows
240 the normal distribution as shown in Fig. 6.

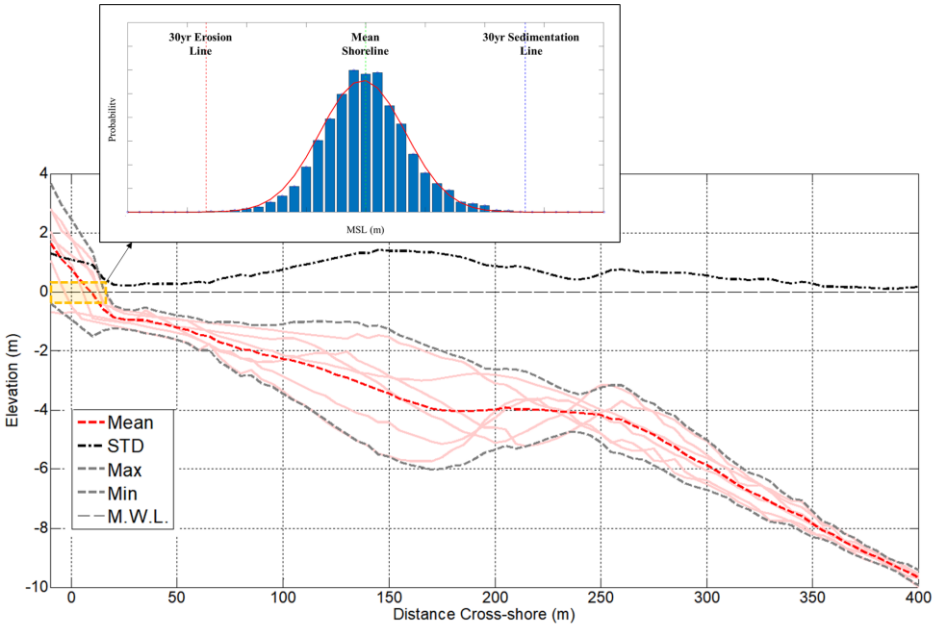

Figure 6: Shoreline variation and its probability distribution at a sandy beach.

https://doi.org/10.5194/nhess-2021-180
Preprint. Discussion started: 8 July 2021

Natural Hazards and Earth System Sciences Discussions

To estimate the maximum width of beach erosion within the specific period, a minimum number of seasonal measurement data are required. If the observed shoreline data follow a normal distribution, then the data can be applied to assess the maximum probable erosion occurring once in n years with a probability of $\frac{1}{4n}$ in a cumulative normal distribution curve. From the cummulative curve of normal distribution, the frequency (F) for a shoreline variable x_F can be determined by,

$$F(x_F) = 1 - \frac{1}{2}[1 + erf\ (\frac{x_F}{\sqrt{2}})]) \quad (16)$$

From Eq. (16), the erosion width (S_{el}) is then calculated for a shoreline variation width (x_F) by,

$$S_{el} = \mu - \sigma x_F \quad (17)$$

where μ is the mean beach width and σ is the standard deviation of the shoreline variation width obtained from the data distribution curve. However, this value represents only the erosion width based on the data collected four times per annum. Unlike measurements taken at regular intervals, different erosion widths may exist at any time when measurements were not taken; hence, the actual value could be larger than that measured and presented in this paper. The eroded beach width due to the *cross-shore sediment retreat potential* with a certain return period (W_e) can be estimated statistically from shoreline observation data,

$$W_e = \sigma x_F \quad (18)$$

The x_F mentioned in Eq. (16) corresponds to the *cross-shore sediment retreat potential* W_e divided by the standard deviation σ of shoreline variation. The frequency $F(x_F)$ corresponds to frequency F_e in the erosion risk potential given in Eq. (5). However, since the shoreline was observed four times a year, it was approximated by multiplying 1.5 to convert it into a daily statistical value of the variation. Table 1 shows the shoreline data variation x_F and the corresponding daily shoreline retreat per frequency F_e.

Table 1: Shoreline data variation x_F and daily shoreline retreat W_e per frequency F_e.

Frequency $F_e\ yr^{-1}$	Shoreline data variable $x_F\ (m)$	Daily shoreline retreat $W_e\ (m)$
1	0.68	1.01
2	1.15	1.73
5	1.65	2.47
10	1.96	2.94
20	2.24	3.36
30	2.40	3.59
50	2.58	3.86
70	2.69	4.04
100	2.81	4.21

https://doi.org/10.5194/nhess-2021-180
Preprint. Discussion started: 8 July 2021


Natural Hazards and Earth System Sciences Discussions

If the method suggested above is not applicable because the amount of shoreline data is not sufficient for statistical analysis, then wave data and sediment grain size (D_{50}) should be used (see method in Kim and Lee, 2018), based on storm-wave-induced erosion on an equilibrium beach profile (Dean, 1977). This gives the total planar area of beach erosion,

$$A_e = W_e L_e \tag{19}$$

where L_e is the shoreline length of the affected beach area.

4. Case Study for Bongpo-Cheonjin Beach

4.1 Study site description

The quantitative interpretation proposed in the present study is applied to the beach erosion problem at Bongpo-Cheonjin Beach (38°15'N, 128°33'E), located in the northeast of Gangwon-do, South Korea, has a small Cheonjin Harbor at its north end and a large Bongpo harbor to its south, as shown in Fig. 7. This crenulate-shaped beach, approximately 1.1 km long, is a closed littoral cell due to the existence of a breakwater (completed in November 2010) for Cheonjin Harbor and a group of natural rocks nearshore (now with a 40-m long groin completed in July 2018 which extends out from the rocks) in the downdrift region. Because beach erosion had often occurred in winter by high waves, three segmented submerged breakwaters of total 490 m in length and one groin of 40 m were installed between November 2017 and November 2019, eventually transforming the beach into a stable embayment.

Application of software MeePaSoL (Lee, 2015) developed to facilitate the use of the parabolic bay shape equation (Hsu and Evans, 1989) indicates the beach is currently close to static equilibrium (using focus points B and C for the updrift and downdrift half of the beach shown in yellow curve, respectively; Fig. 7).

In geomorphic term, Bongpo-Cheonjin beach has received predominant waves from about N47°E direction (drawn by software MeePaSoL); whereas the prevailing wave direction in spring and summer is from N50°E and that in autumn and winter from N30°E in the open sea. Therefore, longshore sediment transport prevails from north to south in autumn and winter, especially during high waves in winter, which had caused severe beach erosion (Fig. 8).

https://doi.org/10.5194/nhess-2021-180
Preprint. Discussion started: 8 July 2021

Natural Hazards and Earth System Sciences
Discussions

Figure 7: Aerial photograph of Bongpo-Cheonjin Beach showing harbors, river, shore protection structures and static bay shapes produced by software MeePaSoL on image courtesy of © Google Earth.

290

Figure 8: Severe beach erosion on Bongpo-Cheonjin Beach during winter high waves on February 19, 2020 (Ministry of Oceans and Fisheries (MOF), 2018).

4.2 Sediment budget reduction in the study site

From a series of 10 aerial photographs of Bongpo-Cheonjin Beach (Fig. 9) spanning over 45 years from 1972 to 2017 (i.e., in
295 July 1972, November 1979, October 1991, June 1997, May 2005, November 2010, May 2011, September 2013, November 2015, and July 2017), data of shoreline position, beach width, and area are extracted at three key locations (A, B, and C along the beach and marked on all sub-panels of Fig. 9 and values tabulated in Table 2). In addition, 37 sets of seasonal shoreline survey data collected during 2008–2017 and NOAA's wave data are applied, with the results presented are graphically in Sect. 3.2 –3.4.

https://doi.org/10.5194/nhess-2021-180
Preprint. Discussion started: 8 July 2021

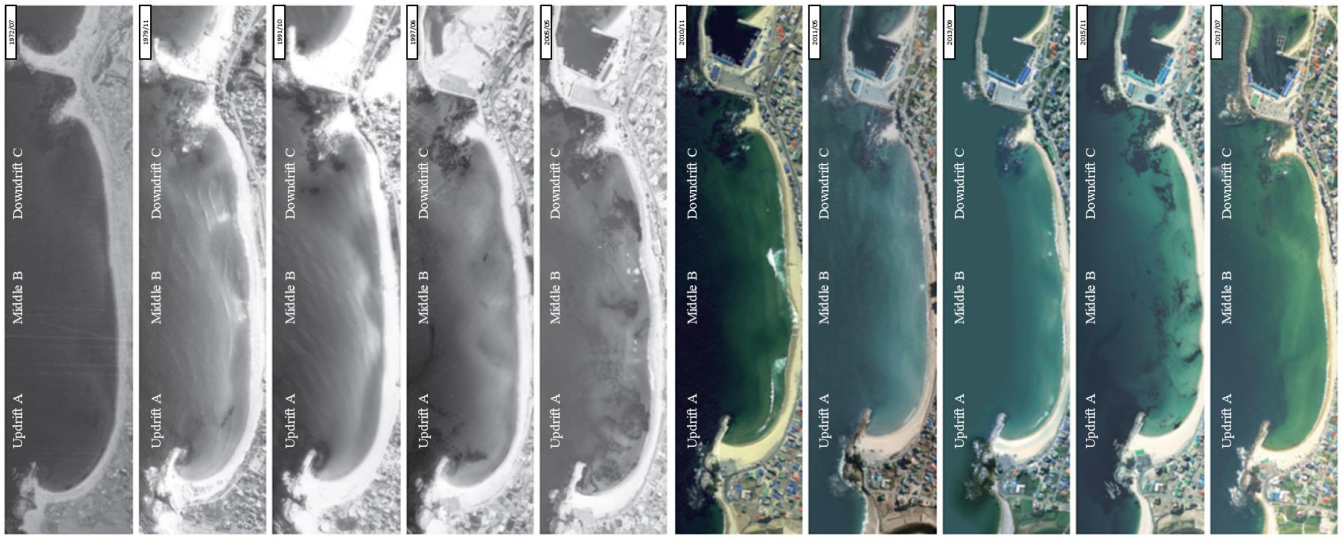

Figure 9: Aerial photographs of Bongpo-Cheonjin Beach by year: (a) 07/1972 (b) 11/1979, (c) 10/1991, (d) 06/1997, (e) 05/2005, (f) 11/2010, (g) 05/2011, (h) 09/2013, (i) 11/2015, and (j) 07/2017 on image courtesy of National Geographic Information Institute (MOF, 2018).

Table 2: Variations in beach area at three key locations of Bongpo-Cheonjin Beach marked on Fig. 9 (MOF, 2018).

MM/YYYY	Months from previous date	Total months from 07/1972	Updrift A (m^2)	Middle B (m^2)	Downdrift C (m^2)
07/1972	1	1	3,266	12,943	5,059
11/1979	89	90	9,699	15,262	6,835
01/1991	143	233	10,986	14,892	5,648
06/1997	68	301	8,969	13,660	6,681
05/2005	95	396	12,279	14,383	4,653
11/2010	66	462	14,194	15,268	5,041
05/2011	7	469	14,980	15,444	4,721
09/2013	28	497	14,416	13,631	5,443
11/2015	26	523	15,144	15,591	5,864
07/2017	20	543	13,669	9,317	3,898

https://doi.org/10.5194/nhess-2021-180
Preprint. Discussion started: 8 July 2021

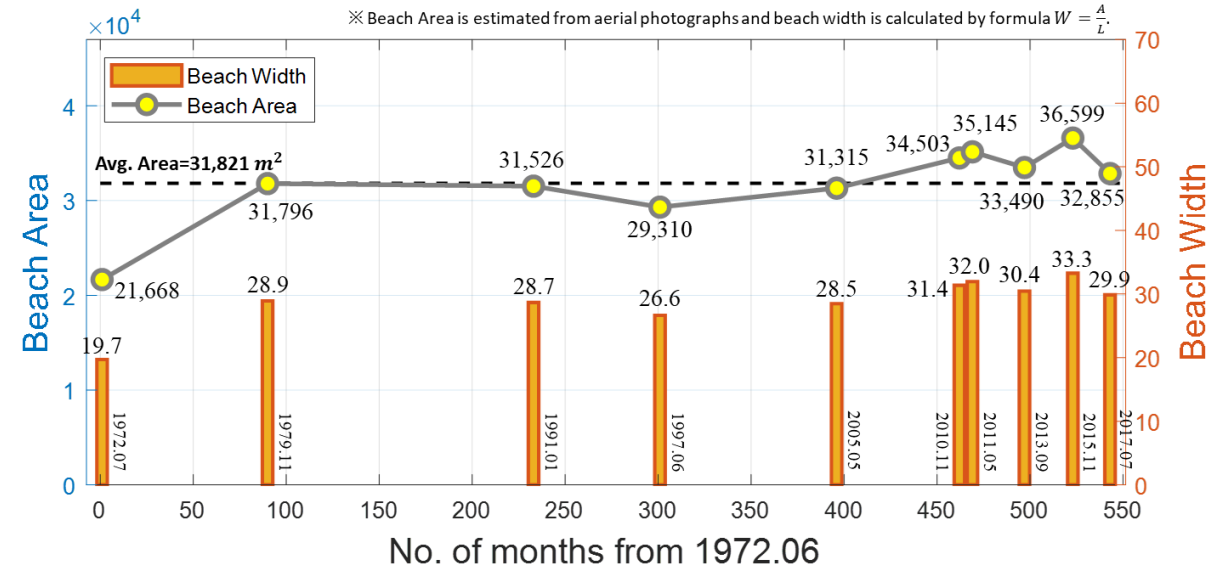

Figure 10: Variations in beach area and width for Bongpo-Cheonjin Beach using aerial photographs.

The beach width extracted from the aerial photograph is the value obtained by dividing the sandy beach area by the length of the shore at the time of the photographing. Therefore, depending on the incidence wave conditions at that time, it may not be able to reflect the effect of shoreline retreat caused by cross-shore sediment transport. The erosion width that occurs at a frequency of one year is about 16.3 m in the Bongpo-Cheonjin beach. It is judged that the range of changes in the beach width in the aerial photograph is within the erosion width.

However, as shown in Fig. 10, since 1979.11, the beach area has been approximately 31,821 m^2 and the beach width has been maintained almost constant at about 28.9 m. Although small underwater barrage was built on Cheonjin river located in the north, there are few the reduction potential in the sediment budget A_c due to its small storage capacity. Then, the eroded beach width due to the *sediment budget reduction potential* to the beach width W_c was also ignored as few.

4.3 Longshore sediment deposition potential caused by the construction of harbor breakwater

As shown in Fig. 11, the beach width of Bongpo-Cheonjin Beach appears to be remained at about 30 m for a long time between 2000 and 2017, in spite of the regional shoreline advance to form a static bay-shape after the construction of the Cheonjin Harbor breakwater. However, shoreline reshaping resulted in sediment deposition in the lee of breakwater and corresponding erosion in the other middle and south of the beach as given in Table 2.

The longshore deposition potential can be approximated by the bay-shape shoreline feature across the whole Bongpo-Cheonjin Beach (Fig. 11). First, the equivalent wave obliquity (β) from the tip of the harbor breakwater can be approximated from the geometry of indentation (a) in relation to the beach length (L_a),

$$\beta = \tan^{-1}\left(\frac{a}{L_a}\right) = \tan^{-1}\left(\frac{150}{850}\right) = 9.68° \quad (20)$$

https://doi.org/10.5194/nhess-2021-180
Preprint. Discussion started: 8 July 2021

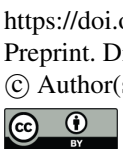

Natural Hazards and Earth System Sciences
Discussions

The *longshore sediment deposition potential* A_d is obtained by substituting the calculated β with β', as indicated in Fig. 5 and Eq. (14),

$$\frac{A_d}{a^2} \cong \frac{28.8}{\beta'} - 0.004\beta = \frac{28.8}{42} - 0.004 \times 9.68 = 0.647 \quad \text{(unit: degree)} \tag{21}$$

For a = 150 m (Fig. 11), Eq. (21) gives A_d = 14,560 m^2. The relationship between β and β' in Eq. (14) can be plotted as shown in Fig. 12 to obtain the dimensionless *longshore sediment deposition potential* ($\frac{A_d}{a^2}$) with values from 0 to 10. Alternatively, the value for A_d/a^2 can be obtained graphically from Fig. 12. By equating A_d^+ with A_d^- (Fig. 11), the amount of beach erosion width W_d is estimated as 17 m by inputting the beach length from the breakwater (L_d = 850 m) into Eq. (15).

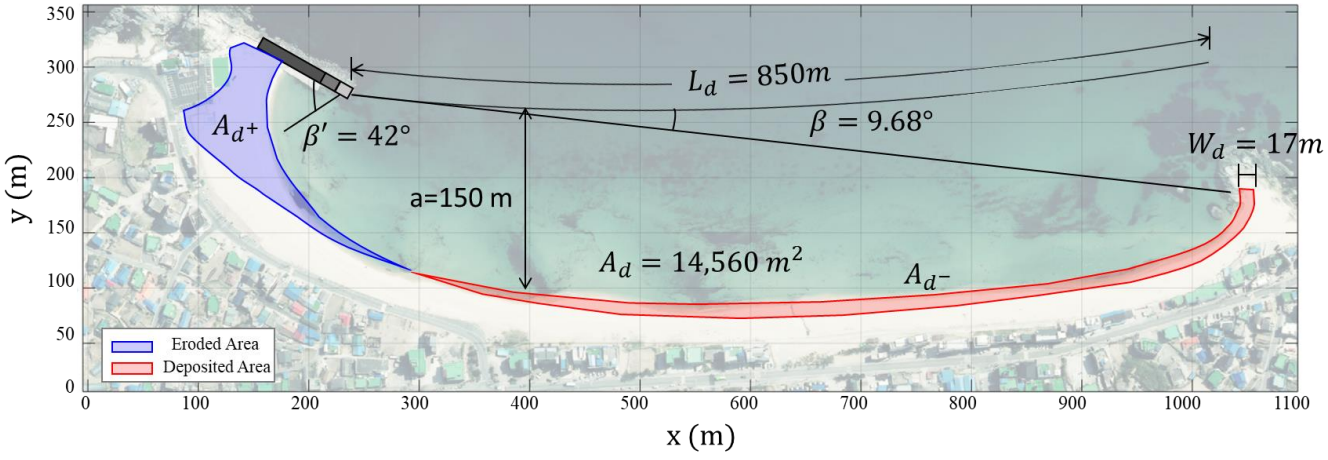

Figure 11: Calculation of longshore sediment deposition potential at Bongpo-Cheonjin Beach on image courtesy of National Geographic Information Institute (MOF, 2020).

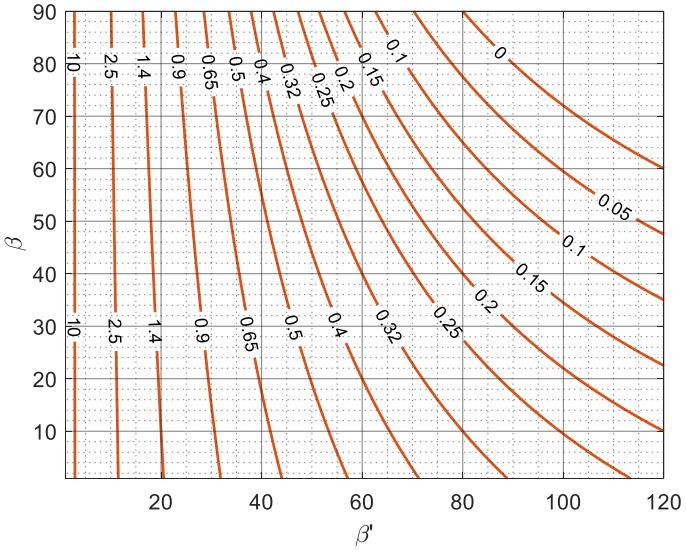

Figure 12: Diagram for determining dimensionless longshore sediment deposition potential ($\frac{A_d}{a^2}$) ranging from 0 to 10 in Eq. (14).

https://doi.org/10.5194/nhess-2021-180
Preprint. Discussion started: 8 July 2021

Natural Hazards and Earth System Sciences
Discussions

4.4 Cross-shore beach retreat due to the high wave incidence

Routine shoreline surveys have been conducted at least four times per annum for beaches in Gangwon-do, South Korea, since the 2000s. Specifically, a total of 37 sets of seasonal data were collected over 10 years from 2008 to 2017 for Bongpo-Cheonjin Beach. These data are plotted and fitted by a normal distribution (Fig. 13) to show local shoreline changes with standard deviation of σ = 5.5 m. Figure 13 also compares alongshore distribution of the mean shoreline and retreated shoreline of 30-year return period from statistical analyses (x_F =3.59). The beach width due to *the cross-shore sediment retreat potential* is evaluated as the value with the range from 5.57 m to 23.16 m (1 $yr \leq F_e \leq 100\ yrs$).

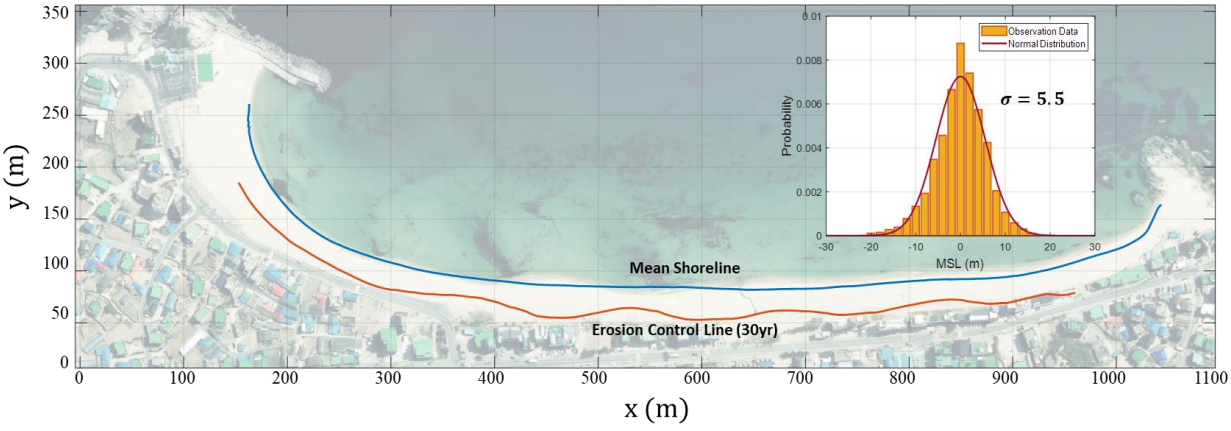

Figure 13: Cross-shore shoreline retreat potential at Bongpo-Cheonjin Beach showing standard deviation σ and mean encroachment σx_F with 30-year return period (within inset) on image courtesy of National Geographic Information Institute (MOF, 2020).

4.5 Erosion risk potential at Bongpo-Cheonjin Beach

The erosion risk potential is obtained by applying the ultimate beach erosion width by each erosion factor to the *encroachment accumulation curve* as given in Chapter 2. Figure 14 shows the *encroachment accumulation curve* according to the distance from the current average shoreline of Bongpo-Cheonjin Beach to the shore. Table 3 shows the encroachment area obtained for each distance of 5m.

The erosion widths of *sediment budget reduction potential* W_c and *longshore sediment deposition potential* W_d are evaluated by 0 m and 17 m, respectively, thus representing the sum of individual components $W_c + W_e$ of 17 m. And the *cross-shore sediment retreat potential* due to high waves W_e is presented in Table 4. The results of shoreline retreat W_t, consequence C_t and risk potential R for each return period are presented in Table 4, where the risk potential R is calculated using Eq. (5). And Figure 14 also shows the consequence C_t per return period T_r ($1/F_e$), which are obtained using the *encroachment accumulation curve*, and figure 15 shows the variation of consequence and the erosion risk potential (ultimate erosion risk) with respect to return periods at Bongpo-Cheonjin Beach.

https://doi.org/10.5194/nhess-2021-180
Preprint. Discussion started: 8 July 2021

Natural Hazards and Earth System Sciences
Discussions

Table 3: Relationship between combined shoreline retreat W_t and consequence C_t for Bongpo-Cheonjin Beach.

$r = W_t\ (m)$	5	10	15	20	25	30	35	40	45	50
$C_t\ (m^2)$	0	0	0	0	181	1,545	3,997	6,951	10,299	13,989

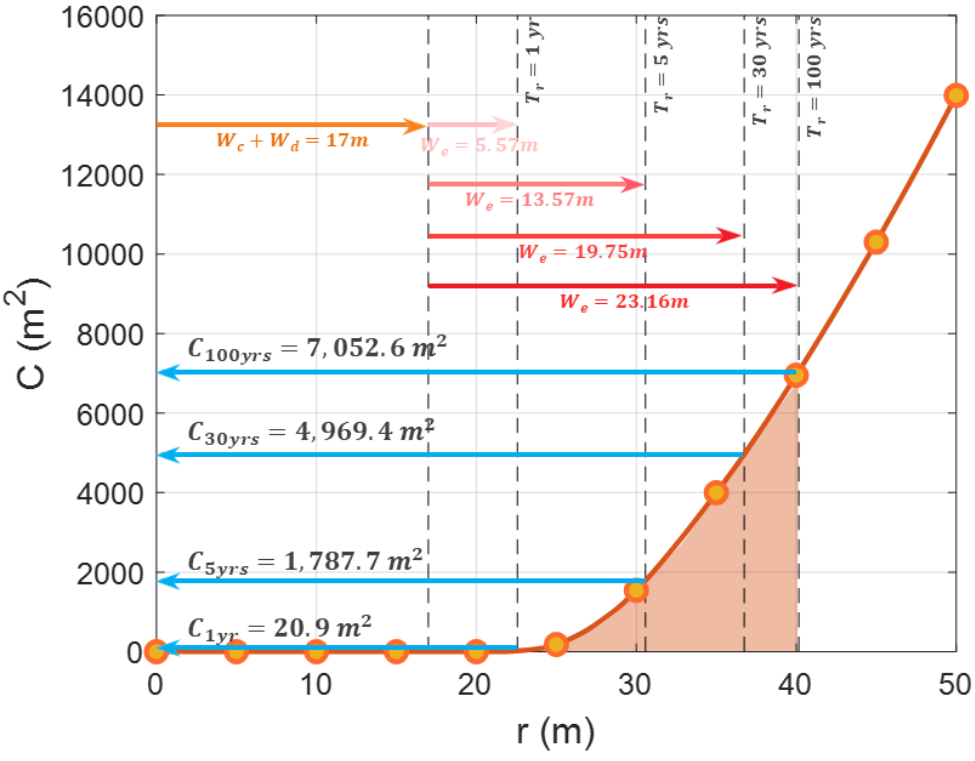

Figure 14: Estimation of the total erosion potential using the encroachment accumulation curve at Bongpo-Cheonjin Beach.

365

Table 4: Erosion risk potential per return period T_r for Bongpo-Cheonjin Beach using the encroachment accumulation curve.

Return period T_r [yr]	Shoreline retreat W_t (W_e) $[m]$	Consequence C_t $[m^2]$	Risk potential R $[m^2]$
1	22.57 (5.57)	20.9	20.9
2	26.49 (9.49)	449.0	224.5
5	30.57 (13.57)	1787.7	357.54
10	33.17 (16.17)	3034.0	303.4
20	35.49 (18.49)	4263.5	213.175
30	36.75 (19.75)	4969.4	165.6467
50	38.25 (21.25)	5861.5	117.23
70	39.19 (22.19)	6440.7	92.01
100	40.16 (23.16)	7052.6	70.526

https://doi.org/10.5194/nhess-2021-180
Preprint. Discussion started: 8 July 2021

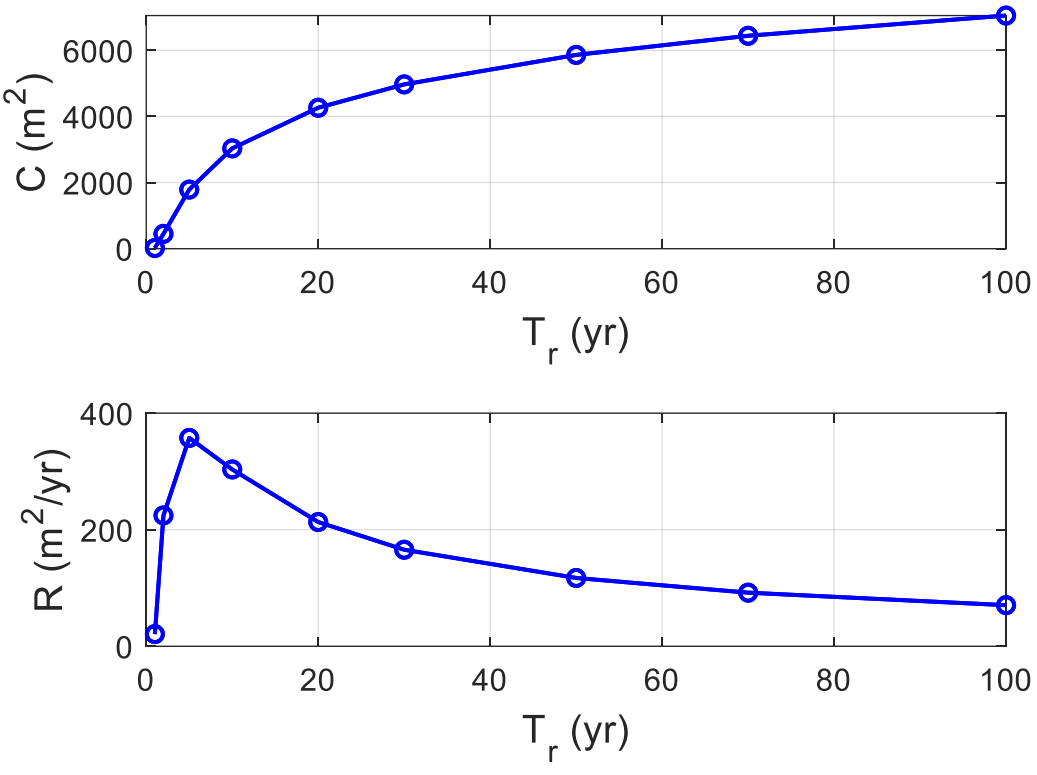

Figure 15: Consequence *C*and risk potential *R* with respect to T_r at Bongpo-Cheonjin Beach.

4. Discussion

In this study, a risk potential was introduced as the meaning of risk when an equilibrium state was reached for a long time, and a quantitative interpretation of risk potential was presented. That is, the risk potential, which is the planar area of the beach that can cause the maximum damage, is calculated excluding the continuous change of the shoreline with time scale. However, even if an erosion factor has occurred, it takes time for erosion to reach equilibrium state. And in order to properly understand the temporal change, it is required to identify more relevant coefficients depending on the target beach. Figure 16 shows the approximate time scale difference in terms of beach width according to three different erosion occurrence elements.

https://doi.org/10.5194/nhess-2021-180
Preprint. Discussion started: 8 July 2021

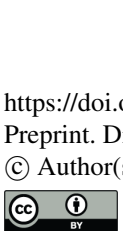

Natural Hazards and Earth System Sciences
Discussions

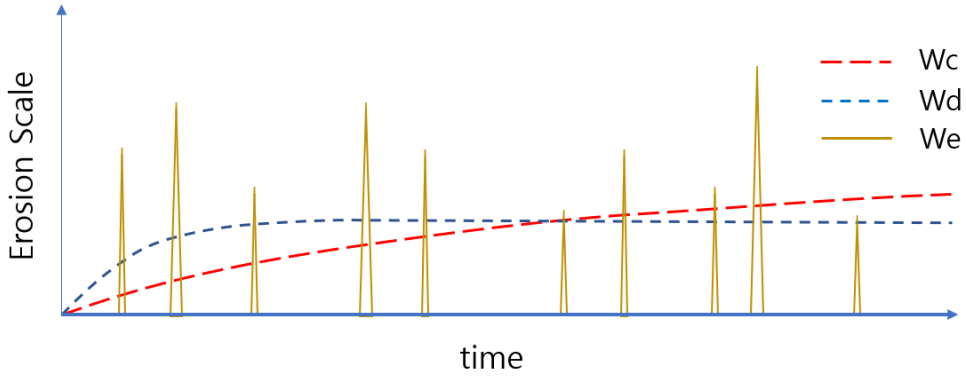

Figure 16: Time scale difference according to erosion occurrence elements.

First, shoreline retreat due to sediment budget reduction occurs as a result of source and sink imbalance in a long-term perspective over several decades. It shows the time-dependent change in the beach area by reflecting the effects of the sand loss rate K_d lost to the offshore and the decrease rate α of the sand flowing into the beach, which are variables representing the effects of source and sink. The theoretical solution is as follows (Lee and Lee, 2020).

$$W_c(t) = \alpha W^o[1 - \exp(-K_c t)] \quad (22)$$

where the sand loss rate K_c is given as a constant value, and it is assumed that the beach area converges to $(1-\alpha)A^o$ due to the decrease rate α of the sediment discharge. Equation (20) shows that the beach area decreases rapidly at the beginning, but converges to 95% or more equilibrium when time passes by $\frac{3}{K}$ yr.

Secondly, the calculation of the erosion width due to longshore sediment transport can be estimated from empirical formulas such as the CERC equation (Shore Protection Manual, 1984). Starting from the angle difference between the initial and equilibrium shoreline angles at the boundary of erosion and deposition caused by shoreline deformation, the temporal width change is obtained by applying exponentially converging angle change to the formula for longshore sediment transport.

$$W_d(t) = W_d^u[1 - \exp(-K_d t)] \quad (23)$$

Here, W_d^u is the ultimate beach width due to longshore sediment transport, and K_d is the rate of change of angle according to time at the junction, and it is estimated by dividing the length of the beach L_d and the vertical littoral height D_s in the formula for longshore sediment transport. The equilibrium shoreline angle due to harbor or coastal structures is obtained based on the PBSE of Hsu and Evans (1989).

Finally, beach erosion due to the transport of cross-shore sediments is a short-term change that occurs over 20~40 days per a storm event. Shoreline retreats when high waves incidence and it recovers again when the wave is extinguished. Yates et al. (2009) confirmed that there is a linear relationship between the location of the shoreline converging to wave energy through field observation. Applying this recoverable process, the shoreline change model proposed by Miller and Dean (2004) can be expressed as the following ODE equation (Kim, 2021).

https://doi.org/10.5194/nhess-2021-180
Preprint. Discussion started: 8 July 2021


Natural Hazards and Earth System Sciences Discussions

$$\frac{dW_e}{dt} = K_e\left(\frac{E_b}{a} - W_e\right) \quad (24)$$

Here, K_e is the beach recovery factor, and E_b is the wave energy at the breaking point. And a is a beach response factor between the wave energy E_b and the mean shoreline. And another factor b, which is proposed by Yates et al. (2009), has little effect, so it is excluded from Eq. (24). If only the value of the beach recovery factor K_e, which has a unique value for each beach with different characteristics, is known, the temporal change of the shoreline according to wave energy can be estimated using Eq. (24).

5. Concluding Remarks

This study presents a quantitative method for identifying the ultimate risk to beach erosion due to the anthropogenic development in watershed, coastal waters and lands, omitting climate change and sea-level rise. The *sediment budget reduction potential* caused by reduction in sediment supply from an upstream river was estimated using a principal of mass conservation (Lee and Lee, 2020). The estimation of *longshore sediment deposition potential* was evaluated by the deformation of a static bay shape (Hsu and Evans, 1989). It is often caused by wave field changes after the construction of harbor breakwater, reclamation projects, and so on. Finally, the *cross-shore sediment retreat potential* by high/storm waves was estimated based on a statistical analysis of shoreline observation data.

The erosion consequence C is obtained from the *encroachment accumulation curve* that accumulates the area to be damaged by the hinterland development of the buffer section based on the average shoreline. Where the planar beach erosion potential obtained in advance is required to evaluate each consequence components. In addition, the erosion risk potential is estimated by multiplying the consequence and frequency. The frequency for A_c and A_d is considered as $1yr^{-1}$, on the other hands, that of A_e is estimated from the statistical characteristics of shoreline survey data.

Through the case analysis for Bongpo-Cheonjin Beach of erosion grade D, Gangwon-do, South Korea, in which a coastal maintenance project was recently conducted, the feasibility of methodology presented in this study was reviewed and the major risks of erosion were quantitatively identified. It was interpreted using a series of aerial photographs taken from 1972 to 2017 and survey data obtained from the erosion rating project started in 2010.

As a result, no dam was built in the watershed of the target beach, small-scale weirs were constructed, so the *sediment budget reduction potential* was judged to be insignificant enough to be difficult to quantitatively express. In addition, the *longshore sediment deposition potential* was evaluated as 17 m after the breakwater of Cheonjin harbor was extended by 40 m. And the *cross-shore sediment retreat potential* was evaluated as the value with the range from 5.57 m to 19.75 m ($1\ yr \leq F_e \leq 30\ yrs$). Therefore, if the shoreline retreat which is the sum of individual components is applied to the *encroachment accumulation curve*, the risk potential is obtained as the value with the range from 20.9 m^2 to 4969.4 m^2 (see Fig. 16 and Table 4). This means that erosion damage to 4,969.4 m^2 areas eroded at least once every 30 years can occur, requiring engineering solutions such as setbacks or beach nourishment projects.

https://doi.org/10.5194/nhess-2021-180
Preprint. Discussion started: 8 July 2021


Natural Hazards and Earth System Sciences Discussions

The erosion risk potential was calculated by applying the standard deviation of 5.5m obtained from the shoreline survey data. As a result, the peak risk potential of 357.54m^2occurred at 5 years recurrence. When the risk assessment method of this study is applied, therefore, it is possible to determine the optimal strategy, comparing the total risk obtained considering the actual damage cost for the erosion section with the average annual cost of the erosion reduction countermeasure method that reduces the consequences or increases the return period.

The methodology proposed here enables the academic and quantitative identification of beach erosion risk and can help to devise engineering measures to eliminate or mitigate the causes of erosion. Although the case analysis of this study is limited, it is necessary to examine the feasibility of the proposed method by steadily applying it to other beaches with severe erosion and to improve it so that it can be applied to more beaches.

Data availability

Not applicable.

Author contributions

Supervision, J.L.L.; Writing—original draft, C.L.; Writing—review & editing, C.L., T.K., S.L. Y.J.Y. and J.L.L.; Data Aquition, C.L., T.K. and S.L. All authors have read and agreed to the published version of the manuscript.

Competing interests

The authors declare no conflicts of interest.

Acknowledgements

This research is part of a project entitled 'Practical Technologies for Coastal Erosion Control and Countermeasure' supported by the Ministry of Oceans and Fisheries, Korea.

References

Ab Razak, M.S., Jamaluddin, N., and Mohd Nor, N.A.Z.: The platform stability of embayed beaches on the west coast of Peninsular Malaysia, JESTEC, 80, 33-42, 2018a.

Ab Razak, M.S. and Mohd Nor, N.A.Z.: Jamaluddin, N. Platform stability of embayed beaches on the east coast of Peninsular Malaysia, JESTEC, 13, 435-448, 2018b.

https://doi.org/10.5194/nhess-2021-180
Preprint. Discussion started: 8 July 2021


Natural Hazards and Earth System Sciences Discussions

Anh, D.T.K., Stive, M.J.F. and Brouwer, R.L.: de Vries, S. Analysis of embayed beach platform stability in Danang, Vietnam, In Proceedings of the 36th IAHR World Congress, The Hague, The Netherlands, 6-28, June-3 July 2015.

Bayram, A., Larson, M. and Hanson. H.: A new formula for the total longshore sediment transport rate, Coastal Eng., 54, 700–710, 2007.

Beven II, J. L., Avila, L. A., Blake, E. S., Brown, D. P., Franklin, J. L., Knabb, R. D., Pasch, R. J., Rhome, J. R., and Stewart, S. R.: Atlantic Hurricane Season of 2005, Mon. Weather Rev., 136, 1109–1173, https://doi.org/10.1175/2007MWR2074.1, 2008.

Bowman, D., Guillén, J., López, L. and Pellegrino, V.: Planview geometry and morphological characteristics of pocket beaches on the Catalan coast (Spain). Geomorphology, 108, 191–199, 2009.

Bray, M. J., Carter, D. J. and Hooke, J. M.: Littoral Cell Definition and Budgets for Central Southern England, Journal of Coastal Research, 11(2), 381-400, 1995.

CERC (Coastal Engineering Research Center): Shore Protection Manual, 4th Ed. U.S. Army Corps of Engineers, Waterways Experiment Station, Coastal Engineering Research Center, U.S. Government Printing Office, Washington, D.C., 1984.

Cooper, N.J.: Engineering Performance and Geomorphic Impacts of Shoreline Management at Contrasting Sites in Southern England. Ph.D. Thesis, University of Portsmouth, Hampshire, England, 1997.

Cooper, N.J. and Pethick, J.S.: Sediment budget approach to addressing coastal erosion problems in St. Ouen's Bay, Jersey, Channel Island, J. Coast. Res., 21, 112–122, 2005. [CrossRef]

Dean, R.G.: Equilibrium beach profiles: U.S. Atlantic and Gulf Coasts, Technical Report, No. 12, Department of Civil Engineering, University of Delaware, 1977.

Dolan, T.J., Castens, P.G., Sonu, C.J. and Egense, A.K.: Review of Sediment Budget Methodology: Oceanside Littoral Cell, California, In Proceedings of the Coastal Sediments '87 (ASCE), Reston, VA, USA, 1289-1304, 23 May 1987.

Edward, B.T., Abby, S., Juan, C.S., Laura, E., Timothy, M. and Rost, P.: Sand mining impacts on long-term dune erosion in southern Monterey Bay, Marine Geology, 229, 1-2, 45-58, 2006.

Foley, M.M., Jonathan, A.W., Andrew, R., Andrew, W.S., Patrick, B.S., Jeffrey, J.D., Matthew, M.B., Rebecca, P., Guy, G. and Randal, M.: Coastal habitat and biological community response to dam removal on the Elwha River, Ecol. Monogr., 87, 552-577, 2017.

González, M., Medina, R. and Losada, M.A.: On the design of beach nourishment projects using static equilibrium concepts: Application to Spanish coast, Coast. Eng., 57, 227-240, 2010.

Harley, M., Armaroli, C., and Ciavola, P.: Evaluation of XBeach predictions for a real-time warning system in Emilia-Romagna, Northern Italy, J. Coast. Res., 64, 1861–1865, 2011.

Herrington, S.P., Li, B. and Brooks, S.: Static Equilibrium Bays in Coast Protection, Marine Engineering Group, Institution of Civil Engineers: London, UK, 2007.

Hsu, J.R.C. and Evans, C.: Parabolic bay shapes and applications, Proceedings of Institution of Civil Engineers, Part 2., Vol. 87, Thomas Telford, London, 557-570, 1989.

https://doi.org/10.5194/nhess-2021-180
Preprint. Discussion started: 8 July 2021

Inman, D. L. and Jenkins, S. A.: The nile littoral cell and man's impact on the coastal zone of the southeastern Mediterranean, Coastal Engineering Proceedings, 1, 19, 109, 1984.

Kamphuis, J.W.: Alongshore transport of sand, Proceedings of the 28th International Conference on Coastal Engineering Conference, ASCE, 2478-2490, 2002.

Kana, T. and Stevens, F. Coastal Geomorphology and Sand Budgets Applied to Beach Nourishment, In Proceedings of the Coastal Engineering Practice '92 (ASCE), Long Beach, CA, USA, 29–44, 9 March 1992.

Kim, T.K.: The Duration-Limited Shoreline Response under a Storm Wave Incidence by the Concept of Horizontal Behavior of Suspended Sediments, Ph.D. Thesis, University of Sungkyunkwan, Suwon, South Korea, 2021.

Kim, T. K. and Lee, J. L.: Analysis of shoreline response due to wave energy incidence using an equilibrium beach profile concept, J. Ocean Eng. Technol., 2(1), 55–65, 2018.

Komar, P.D. and Inman D.L.: Longshore and transport on beaches, J. Geophys. Res., 75, 5914–5927, 1970.

Kunz, M., Mühr, B., Kunz-Plapp, T., Daniell, J. E., Khazai, B., Wenzel, F., Vannieuwenhuyse, M., Comes, T., Elmer, F., Schröter, K., Fohringer, J., Münzberg, T., Lucas, C., and Zschau, J.: Investigation of superstorm Sandy 2012 in a multidisciplinary approach, Nat. Hazards Earth Syst. Sci., 13, 2579–2598, https://doi.org/10.5194/nhess-13-2579-2013, 2013.

Lee, J.L.: MeePaSoL: MATLAB-GUI based software package, Sungkyunkwan University, SKKU Copyright No. C-2015-02461, 2015.

Lee, S. and Lee, J. L.: Estimation of background erosion rate at Janghang Beach due to the construction of Geum estuary tidal barrier in Korea, J. Mar. Sci. Eng., 8, 551, 2020.

Lim, C., Lee, J. and Lee, J. L.: Simulation of bay-shaped shorelines after the construction of large-scale structures by using a parabolic bay shape equation, J. Mar. Sci. Eng., 9, 43, 2021.

McCall, R. T., Van Thiel de Vries, J. S. M., Plant, N. G., Van Dongeren, A. R., Roelvink, J. A., Thompson, D. M., and Reniers, A. J. H. M.: Two-dimensional time dependent hurricane overwash and erosion modeling at Santa Rosa Island, Coast. Eng., 57, 668– 683, https://doi.org/10.1016/j.coastaleng.2010.02.006, 2010.

Miller, J. K. and Dean, R. G.: A simple new shoreline change model, Coastal Eng., 51(7), 531–556, 2004.

Ministry of Oceans and Fisheries (MOF): Development of Coastal Erosion Control Technology, Ministry of Oceans and Fisheries R&D Report, 2020.

Ministry of Oceans and Fisheries (MOF): Research on the Actual Conditions of Coastal Erosion, Ministry of Oceans and Fisheries R&D Report, 2018.

Montaño, J., Coco, G., Antolínez, J.A.A., Beuzen, T., Bryan, K.R. Cagigal, L. Castelle, B., Davidson, M.A., Goldstein, E.B., Ibaceta, R., Idier, D., Ludka, B.C., Masoud-Ansari, S., Méndez, F.J., Murray. A.B., Plant, N.G., Ratliff, K.M., Robinet, A., Rueda, A., Sénéchal, N., Simmons, J.A., Splinter, K.D., Stephens, S., Townend. I., Vitousek. S., and Vos. K.: Blind Testing of Shoreline Evolution Models, Scientific Reports, 10, 2137, 2020.

https://doi.org/10.5194/nhess-2021-180
Preprint. Discussion started: 8 July 2021

Pelnard-Considere, R.: Essai de Theorie de l'Evolution des Formes de Rivage en Plages de Sable et de Galets, Journées de L'hydraulique, 4, 289–298, 1957.

Pethick, J.S.: Geomorphological Assessment Draft Report to Environment Committee, Environment Committee, St. Ouen's Bay, JE, USA, 1996.

Roelvink, D. and Reniers, A.: Advances in Coastal and Ocean Engineering, Vol. 12, A Guide to Modeling Coastal Morphology, 2012.

Roelvink, D., Reniers, A., van Dongeren, A., van Thiel de Vries, J., McCall, R., and Lescinski, J.: Modelling storm impacts on beaches, dunes and barrier islands, Coast. Eng., 56, 1133–1152, https://doi.org/10.1016/j.coastaleng.2009.08.006, 2009.

Sanuy, M., Duo, E., Jäger, W.S., Ciavola, P. and Jiménez, J. A.: Linking source with consequences of coastal storm impacts for climate change and risk reduction scenarios for Mediterranean sandy beaches, Nat. Hazards Earth Syst. Sci., 18, 1825–1847, https://doi.org/10.5194/nhess-18-1825-2018, 2018.

Silveira, L.F., Klein, A.H.F. and Tessler, M.G.: Headland-bay beach platform stability of Santa Catarina State and the northern coast of São Paulo State, Braz. J. Oceanogr., 58, 101–122, 2010.

Spencer, T., Brooks, S. M., Evans, B. R., Tempest, J. A., and Möller, I.: Southern North Sea storm surge event of 5 December 2013: Water levels, waves and coastal impacts, Earth-Sci. Rev., 146, 120–145, https://doi.org/10.1016/j.earscirev.2015.04.002, 2015.

Swart, D. H.: Offshore sediment transport and equilibrium beach profiles, Tech. Rep. Publ. 131, Delft Hydraulics Lab, Delft, Netherlands, 1974.

Thomas, T., Williams, A.T., Rangel-Buitrago, N., Phillips, M. and Anfuso, G.: Assessing embayment equilibrium state, beach rotation and environmental forcing influences, Tenby Southern Wales, UK. J. Mar. Sci. Eng., 4, 30, 2016.

USACE: Coastal Engineering Manual (online). US Army Corps of Engineers, Washington, D.C., 2002.

Van Verseveld, H. C. W., Van Dongeren, A. R., Plant, N. G., Jäger, W. S., and den Heijer, C.: Modelling multi-hazard hurricane damages on an urbanized coast with a Bayesian Network approach, Coast. Eng., 103, 1–14, https://doi.org/10.1016/j.coastaleng.2015.05.006, 2015.

Wang, H., Dalrymple, R. A., and Shiau, J. C.: Computer Simulation of Beach Erosion and Profile Modification due to Waves, Proc. 2nd Annual Symp. of Waterways, Harbours and Coastal Engng. Div. ASCE on Modeling Techniques(Modeling '75: San Franc), 2, 1369-1384, 1975.

Warrick, J.A., Stevens, A.W., Miller, I.M., Harrison, S.R., Ritchie, A.C., and Gelfenbaum, G.: World's largest dam removal reverses coastal erosion, Sci. Rep., 1–12, 2019.

Wright, L.D., Short, A.D. and Green, M.O.: Short-term changes in the morphologic states of beaches and surf zones: an empirical model. Mar. Geol., 62: 339-364, 1985.

Yates, M.L., Guza, R.T. and O'Reilly, W.C.: Equilibrium shoreline response: observations and modeling, Journal of geophysical research, 114(C9), C09014, 2009.

Yu, J.T. and Chen, Z.S.: Study on headland-bay sandy cast stability in South China coasts, China Ocean Eng., 25, 1, 2011.